MPD THRUSTER EXHAUST VELOCITY MEASUREMENT USING INJECTED PLASMA WAVES

K.D. Diamant*, D.L. Tilley°, E.Y. Choueiri¿, A.J. Kelly◊, R.G. Jahn∇
Electric Propulsion and Plasma Dynamics Laboratory
Princeton University
Princeton, NJ 08544

Abstract

Ion flow velocity vector measurements have been obtained in the exhaust of a 30kW steady state MPD thruster using a technique called Phase Flow Velocity Deconvolution. At a location 2 cm downstream of the nozzle exit plane and at 1.5 and 2 cm radially off thruster centerline the velocity has been measured to be approximately 6200 m/s at an angle near 45° with respect to the centerline. The error associated with these measurements is approximately 20%. The flow velocity magnitude is consistent with thrust measurements obtained by Myers using the same thruster under similar operating conditions.

Introduction

This paper is primarily intended to provide a description of a new technique for measuring plasma thruster exhaust velocity. The technique is capable of producing detailed velocity profiles, but has been used to obtain point measurements for the preliminary evaluation tests of this study.

The measurement technique is an outgrowth of Edgar Choueiri's Plasma Wave Experiment [1], in which the propagation velocity of injected plasma waves in a MW level pulsed thruster plume is inferred from disturbance spectra recorded at different locations in the plasma. To measure the plasma dispersion relation Choueiri separated the bulk flow velocity from the wave disturbance (phase) velocity. His method for doing so has been adapted for use in the steady state 30kW thruster.

In the past, velocity measurements have been made with a probe technique called Time of Flight [2]. This technique determines the time required for a disturbance to travel from one probe to another by comparing common features of their current collection time histories. This technique is only useful when the phase velocity of the waves composing the disturbance is much less than the plasma flow velocity. Otherwise, the fact that the disturbance is propagating through the plasma as well as convecting with it must be taken into account.

Choueiri's technique determines the wave phase velocity, the plasma flow velocity, and the flow direction. Current collection histories are examined in the frequency domain, allowing the effect of wave dispersion (the variation of wave phase velocity with frequency) to be taken into account. The technique also has the potential to provide a large number of estimates of the (frequency independent) flow velocity in a single run.

Choueiri has named the technique Phase Flow Velocity Deconvolution (PFVD). The principal advantage of this technique is the simplicity afforded by the use of Langmuir probes. Its principal disadvantage is difficulty in interpreting the raw data.

Harmonically rich, broad band waves are excited in the plasma by varying the potential on a Langmuir double probe that

---

*Graduate Student, Department of Mechanical and Aerospace Engineering Member AIAA, ASME

°Graduate Student, Member AIAA Presently at Phillips Laboratory, Electric Propulsion Group, Edwards AFB, Calif.

¿Research Associate Electric Propulsion and Plasma Dynamics Laboratory

◊Manager and Senior Research Engineer Electric Propulsion and Plasma Dynamics Laboratory Member, AIAA

∇Professor, Department of Mechanical and Aerospace Engineering Fellow, AIAA is biased into ion saturation and is aligned perpendicular to the flow. The disturbance produced by this "emitter" is small and propagates linearly with no mixing of the frequency components contained in the disturbance. Receivers (other Langmuir probes also biased into ion saturation) detect the waves as variations in collected current. It is assumed that these variations are due to ion density variations produced by waves originating at the emitter. When a high degree of correlation exists between frequency spectra recorded by receivers at different spatial locations, each frequency component of a given spectrum can be considered to be directly related to the same component in the other spectra. Comparison of the phase angles of each component yields the time delays between the appearance of that component at the various receiver locations. If it is assumed that the wave disturbance (phase) velocity is isotropic, these time delays, plus the known geometry of the probe array permits the phase and flow velocity to be determined.

The assumption of isotropic phase velocity is difficult to justify. Anisotropy due to gradients in density, temperature, and magnetic field strength may be present since the scale length for those gradients in the near plume (within a few centimeters of the thruster exit plane) of the thruster has been shown [3] to be of the same order as the size of the probe. The angle of propagation with respect to the magnetic field is probably not a strong contributor to anisotropy since, if the magnetic field in the near plume retains the purely azimuthal geometry of the interelectrode region, it is likely that waves being generated and detected by the probe will all be travelling at an angle near 90° to the magnetic field. As shown in reference 1 (p. 97), the angle of propagation with respect to the current velocity may also influence the phase velocity, and the direction of the current velocity is not well known. Fortunately, the ratio of the electron-ion collision frequency to the dominant lower hybrid frequency is around 100 in the near plume, so that collisions may significantly isotropize propagation [1] (p.97). We make the assumption that this is happening.

The success of this technique requires that all of the receivers be affected by the disturbances created at the emitter. In cases where the flow velocity exceeds the wave phase velocity, there will be a limitation on the size of the flow angle observable with the probe due to the presence of a "Mach cone". This turned out not to be a problem for us since we measured phase velocities in excess of the flow velocity.

The Experiment

The experiment reported here was conducted in the Princeton 30 kW steady state thruster facility. This facility and the pendulum-arm system used to position the probe in the thruster exhaust are described in reference 3. A schematic of the pendulum arm and thruster is shown in Figure 1. The size of the probes in the figure is typical of the probes used in this experiment, but their number and configuration is not shown correctly.

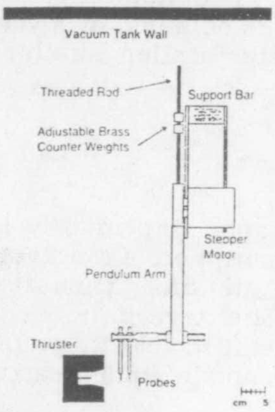

Figure 1: Scale Drawing of Thruster and Pendulum Arm

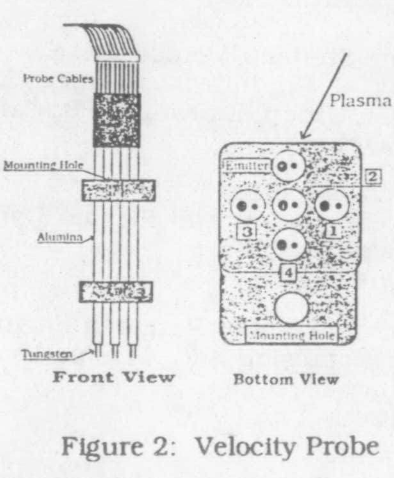

Figure 2: Velocity Probe

Figure 2 shows the probe used to make the velocity measurements. It is composed of five Langmuir double probes in the form of a cross: an emitter and four downstream receivers. The separation between the ion collecting wires of any two probes, as measured along an arm of the cross, is 0.5 cm. The separation between the ion annd electron collecting wires on each probe is about 1 mm. The probe wires are 0.5 cm long segments of 250 and 750 μm diameter tungsten, the thicker wire being used as the ion collector. The alumina sleeves are approximately 3 mm in diameter. This choice of diameter for the alumina was a poor one since the ion-ion mean free path has been estimated to be on the order of a centimeter in the near plume. It is thus difficult to be assured that the probe is not influencing the ion flow velocity. Double probes are used because it is easy to drive a double probe into ion saturation. For equal ion and electron temperatures, the ion collector will sit below floating potential by almost the entire value of the bias applied to the probe. In the experiment a bias of 20 volts, provided by Kepco 36V, 3A power supplies, is typically applied to the receivers. This is adequate to insure that they are in ion saturation since the electron temperature in the exhaust is around 2 eV.

The emitter is similarly biased into ion saturation and is additionally fed a harmonically rich signal. This oscillating signal is a combination of 10 square waves with frequencies ranging from 1 to 100 kHz. The selection of the frequency range used to drive the emitter is governed by the desire to excite a disturbance which will be detectable above background noise. Choueiri [1] has shown that for MPD thruster plasmas the waves with the largest temporal growth rate occur in the neighborhood of the lower hybrid frequency, which is expected to be on the order of 10 or 100 kHz for our plama (argon with T_e of 1 to 3 eV, n_e of 10^{12} to 10^{13} cm^{-3}, B of 1 to 10 gauss). The signal generator (Motorola MC14411 bit rate generator) is designed to output the sum of the 10 square waves after they have been differentiated. Figure 3 is a typical emitter power spectrum. The signal is purposely attenuated towards high frequencies to reduce aliasing error from signals with frequencies above the Nyquist frequency of the digitally recording oscilloscopes, which was set at 1 MHz for these experiments.

Figure 4 is a block diagram of the electronics attached to each receiver. The emitter is also shown. Tektronix CT-

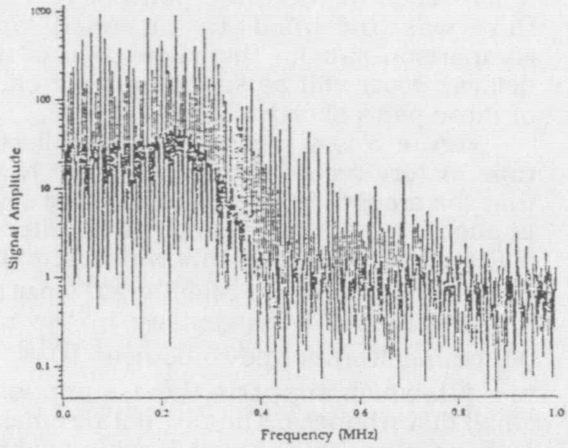

Figure 3: Emitter Power Spectrum

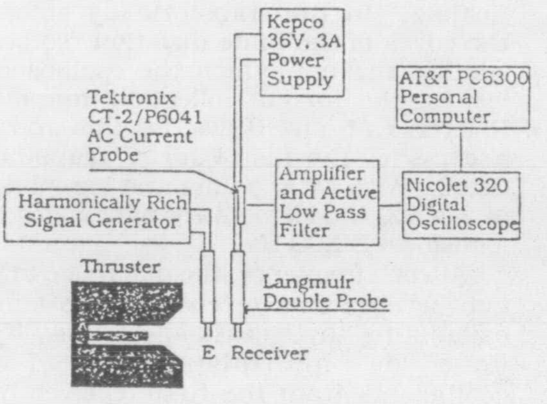

Figure 4: Receiver Electronics

2/P6041 AC current probes reacted to the fluctuations in collected current. The current probe provides 1mV/mA over a bandwidth of 10 kHz to 50 MHz. This signal is amplified by a factor of 100 and filtered by an active, second order low pass filter of the VCVS type [4] to reduce aliasing error. The signal is then recorded by a dual channel Nicolet 320 digital oscilloscope. The oscilloscope is triggered to record 4000 points at a sampling rate of 2 MHz by an AT&T PC6300 personal computer. A total of three dual-channel oscilloscopes was required for the four receivers. The extra oscilloscope was necessary because it was found that there was often a time delay between the triggering of separate scopes that was on the order of the delays that were expected to be measured. To eliminate this problem, a separate scope was used to record each of the three pairs of receivers that was intended to be used as a comparison pair for the calculation of time delays. More will be said about the choice of these pairs shortly.

Figure 5 is a typical current collection time history recorded at receiver 2. Notice that the amplitude of the disturbance signal is about 1 mA. Assuming purely thermal collection of 2 eV ions this would require a disturbance density of roughly 10^{17} per m^3. The undisturbed ion density in the near plume has been found to be near 10^{19} per m^3 [3], which supports the assumption of small disturbances. The raw data from each receiver is multiplied by a Hanning window and then fast Fourier transformed. Figure 6 is typical of spectra recorded at receivers 2 and 3. The Hanning window reduces "leakage" in the transform by smoothing the edges of the finite duration rectangular window through which the oscilloscope is viewing the current collection time history. References 5 and 6 discuss this and other aspects of the fast Fourier transform in detail. With 4000 points at a sampling rate of 2 MHz, the elementary bandwidth of the transform is 500 Hz.

At each frequency, the difference in phase between any two receivers is obtained by calculating their cross-spectrum. This is done by multiplying the Fourier coefficients from the first receiver by the complex conjugate of the Fourier coefficients from the second receiver. The phase angles of the resulting set of complex numbers (known as the cross-spectrum) will be the phase differences between the two receivers at each frequency provided by the transform. It is possible to reduce the statistical error associated with the calculation of these phase angles by smoothing (averaging) the cross-spectrum over several adjacent elementary frequency bands [6]. Tilley has shown that this averaging process will reduce the scatterf in the calculation of phase angles without affecting the mean values of those angles [7]. In this analysis, groups of 30 adjacent frequency bands in the raw cross-spectrum were averaged over, with the result being assigned to the central frequency of the group. Phase angles are calculated from the resulting averaged cross-spectrum. The time delay between the appearance of a given frequency component at the receivers is determined by dividing the phase difference by 2π times the

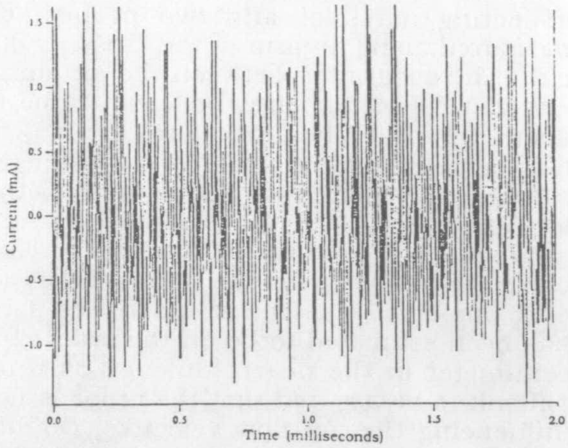

Figure 5: Current Collection Time HIstory

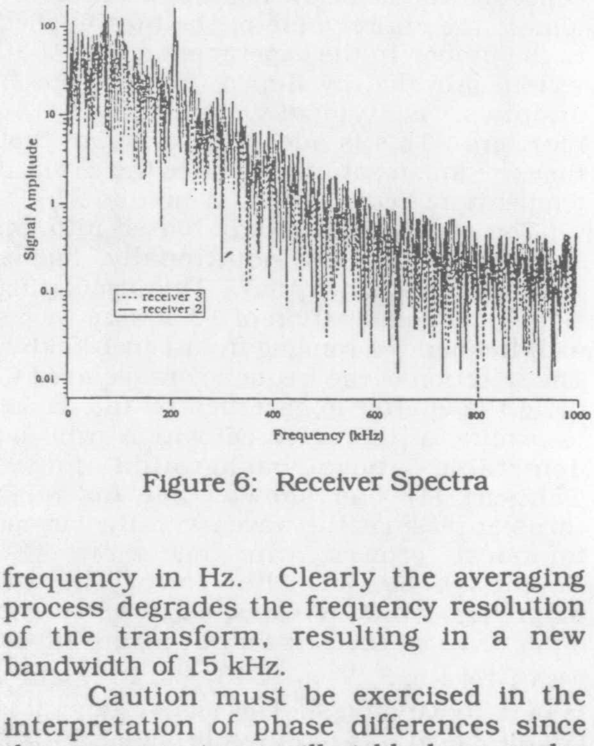

Figure 6: Receiver Spectra

frequency in Hz. Clearly the averaging process degrades the frequency resolution of the transform, resulting in a new bandwidth of 15 kHz.

Caution must be exercised in the interpretation of phase differences since the cross-spectrum will yield phase angles between 0 and 2π while it is quite possible that the true phase difference may exceed 2π. There is no absolute method of determining whether the phase angle has "wrapped around" past 2π. However, Choueiri [1] has shown that the most unstable waves in MPD thruster plasmas have a wavenumber given approximately by kr_{ce} = 0.1, where r_{ce} is the electron Larmor radius. This translates to a wavelength on the order of centimeters, which is larger than the probe. While this fact in no way guarantees that wraparound will not occur (since the time delays are dependent on the flow velocity and flow angle as well as the phase velocity), in this experiment it is always initially assumed that there is no wraparound. If this assumption leads to a nonsensical answer, then single wraparound is considered.

Spurious phase shifts can be introduced by the power supplies, recording equipment, amplifiers, filters, and even the cables attached to the probes. Prior to data collection, a series of mock experiments were performed in the absence of the plasma with the probes short circuited. These experiments guided the matching and tuning of the equipment to minimize the unwanted phase shifts. These were generally held to less than a percent of the phase shifts measured in the actual experiment.

A useful quantity to be calculated in the comparison of two receiver spectra is the coherence spectrum. It is defined as the amplitude of the averaged cross-spectrum divided by the square root of the product of the averaged auto-spectra. The auto-spectrum of each receiver is calculated by multiplying each Fourier coefficient by its complex conjugate. The averaging procedure is just that described above for the cross-spectrum (each auto-spectrum is calculated and then averaged over 30 adjacent frequency bands). Coherence is an indication of the degree of correlation between signals and ranges in value from 0 to 1. Figure 7 is a blow up of a range of frequencies in Figure 6 over which the coherence is near 1. The signals recorded at the two receivers are clearly very similar. Only data showing high coherence is acceptable in this experiment since meaningful information can only be obtained when all receivers are subject to the same disturbance.

The Time Delay Equations

With measured time delays between the appearance of waves at the various receivers in an array of known geometry it is possible to deduce the ion flow velocity (v_f), wave phase velocity (v_ϕ), and angle of

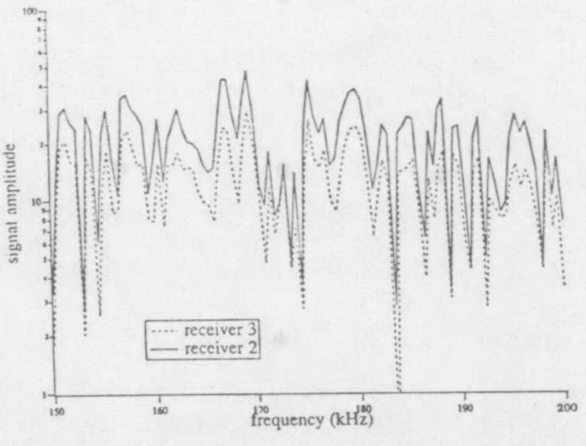

Figure 7: Illustration of Highly Coherent Signals

the flow velocity with respect to the thruster centerline (θ). The use of four receivers and one emitter in a cross configuration allows the measurement of three independent time delays (four receivers give three independent comparisons). Each time delay is described by one equation, derived from the receiver array geometry, involving the three quantities of interest. The emitter is not used as a point of comparison since the spectrum recorded there consistently showed low coherence in comparisons with receiver spectra.

Ray tracing for the geometry of Figure 8 permits the signal time delays Δt to be related to v_f, v_ϕ, and θ. The equation shown on the figure is for the time delay between production of a disturbance at the emitter and its appearance at receiver 1. One of these equations can be written for each of the four receivers. The equations are quadratic and thus can be solved easily for the time delays. These time delays are not directly useful because they are referenced to the emitter, and the emitter has shown consistent difficulty with coherence as mentioned above. To eliminate the emitter as a reference, differences between the time delays are taken. For instance, the time it takes for a disturbance to go from the emitter to receiver 2 may be subtracted from the time it takes to go from the emitter to receiver 1, producing a new time delay indicative of the difference between the times of arrival at the two receivers. This time delay may be measured by comparison of the receivers only.

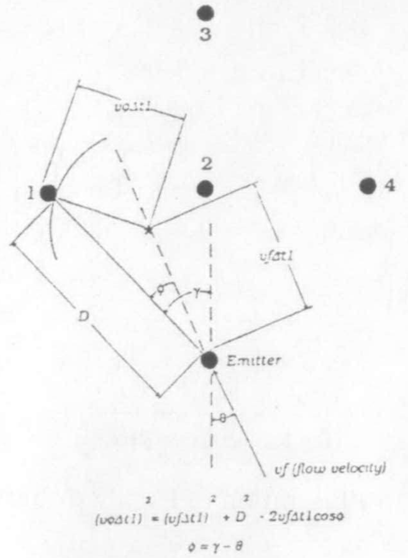

Figure 8: Ray Diagram for Time Delay Equations

The three time delays that were chosen to be measured are those between receivers 1 and 2 (call it Δt_{12}), 2 and 3 (Δt_{23}), and 1 and 4 (Δt_{14}). The equations relating these time delays to v_f, v_ϕ, and θ are as follows :

$$\Delta t_{12} = [(dv_f)/A][-2^{1/2}\cos\phi + \cos\theta + \{2[(v_\phi/v_f)^2 - (\sin\theta)^2]\}^{1/2} - \{(v_\phi/v_f)^2 - (\sin\theta)^2\}^{1/2}]$$

$$\Delta t_{23} = [(dv_f)/A][\cos\theta - \{(v_\phi/v_f)^2 - (\sin\theta)^2\}^{1/2}]$$

$$\Delta t_{14} = [2^{1/2}(dv_f)/A][-2^{1/2}\sin\theta + \{(v_\phi/v_f)^2 - (\sin\theta)^2\}^{1/2} - \{(v_\phi/v_f)^2 - (\sin\gamma)^2\}^{1/2}]$$

where: $A = v_\phi^2 - v_f^2$

$\phi = \gamma - \theta$

γ = angle specified by probe design (see Fig. 8)

Solving the Time Delay Equations

Attempts were made to solve the equations both in closed form and with numerical routines (specifically subroutine DNEQNJ from the IMSL library [8] and Mathematica [9]) designed to solve simultaneous nonlinear equations. It was found that there is no closed form solution, and the numerical solvers were found to be so sensitive to the required initial estimate of the root as to render themselves impractical. A more successful approach was based on converting the equations into a polynomial form, and using a standard root finding routine.

The Δt_{23} equation may be solved directly for v_ϕ with the result:

$$v_\phi = \{(d/\Delta t_{23})^2[2\Delta t_{23} v_f \cos\theta/d + 1] + v_f^2\}^{1/2}$$

This result is used to eliminate v_ϕ from the Δt_{14} equation, and the following fourth order polynomial in v_f with coefficients dependent on θ is obtained:

$$Av_f^4 + Bv_f^3 + Cv_f^2 + Dv_f + F = 0$$

where:

$A = (T\cos\theta/E^4)(2\sin\theta + T\cos\theta - (\sin 2\theta)(2T^2\cos\theta + 3T\sin\theta) - 4\sin^3\theta - T^3\cos^3\theta)$

$B = (1/E^3)(T\sin\theta + T^2\cos\theta + (\sin 2\theta)[(2-3T^2)\sin\theta + T(4-3T^2)\cos\theta] - 2T\sin^3\theta + 2T^2(2-T^2)\cos^3\theta)$

$C = (1/E^2)[(2-(3/2)T^2)\sin^2\theta + T^2(6-(3/2)T^2)\cos^2\theta + T(4-(3/2)T^2)\sin 2\theta + (1/4)T^2]$

$D = (T/E)[(2-(1/2)T^2)\sin\theta + T(3-(1/2)T^2)\cos\theta]$

$F = (T^2/2)(1-T^2/8)$

$E = d/\Delta t_{23}$

$T = \Delta t_{14}/\Delta t_{23}$

d = probe spacing = 5 mm (not same as D in Figure 8)

The solution procedure is: assume a value for θ and solve for the four roots of the v_f polynomial. The IMSL subroutine DZPORC was used to solve the polynomial. For each real positive v_f calculate v_ϕ (from the Δt_{23} equation) and use the assumed value of θ to calculate Δt_{12}. Values of θ ranging from 0 to 90° are checked at one degree increments and the root is determined as the values of θ and v_f that give the smallest difference between the calculated and measured values of Δt_{12}.

While the above polynomial-solving technique outperforms general nonlinear numerical solvers, it lacks adequate sensitivity for consistently good performance. The trouble is that the time delays are very small numbers (of order 10^{-5} to 10^{-7} seconds), creating attractive "roots" for the polynomial solver which are significantly different (20% or more) from the best root. When it was suspected that the polynomial solver was having problems, a final brute force attack was made by giving a computer the three equations in their original form and having it run through a given set of values of v_f, v_ϕ, and θ and report the combination which yields the smallest percentage error between measured and calculated time delays.

Results

Figures 9 through 11 are typical coherence, phase difference, and time delay spectra obtained from a comparison of receivers 2 and 3. Similar information from the other receivers has produced the following velocity measurements at operating conditions of 700 A and 690 A respectively with an argon mass flow of 8 mg/s: v_f = 6200 m/s, θ = 45°, v_ϕ = 6400 m/s for Δt_{14} = Δt_{12} = 3.5 $\cdot$ 10^{-6} seconds and Δt_{23} = -5.6 $\cdot$ 10^{-7} seconds at 2 cm downstream of the thruster exit plane and 2 cm radially off the thruster centerline. v_f = 6200 m/s, θ = 50°, v_ϕ = 6700 m/s for Δt_{14} = 3.0 $\cdot$ 10^{-6}, Δt_{12} = 2.8 $\cdot$ 10^{-6}, and Δt_{23} = -5.8 $\cdot$ 10^{-7} seconds was found at the same axial location but 1.5 cm radially off the thruster centerline. Although this technique has the potential to record a velocity measurement at each individual frequency in the receiver spectra (yielding the dispersion relation of the plasma through the variation of v_ϕ with frequency), and hence produce many estimates of the flow velocity in a single run, what was done to produce the values given above was to choose a frequency with exceptionally high coherence for all of the receivers and use it to make just one velocity estimate. For the 700 A run the time delays were taken from data near 300 kHz. Time delays for the 690 A run were taken from data at approximately 375 kHz.

Sources of uncertainty for the velocities are the time delays and the measurement of the distance between the receivers. The time delays are composed of a phase difference and a frequency. For data with

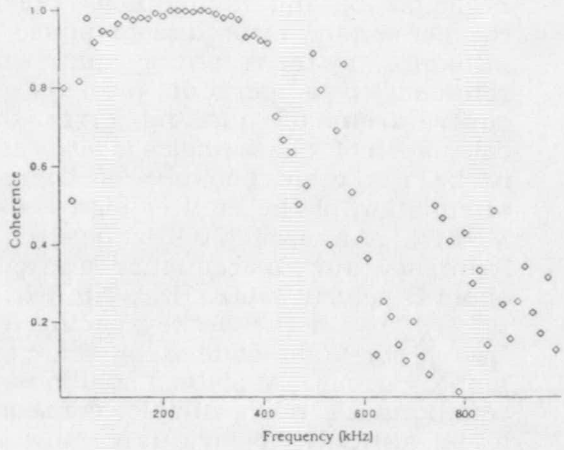

Figure 9: Coherence Spectrum

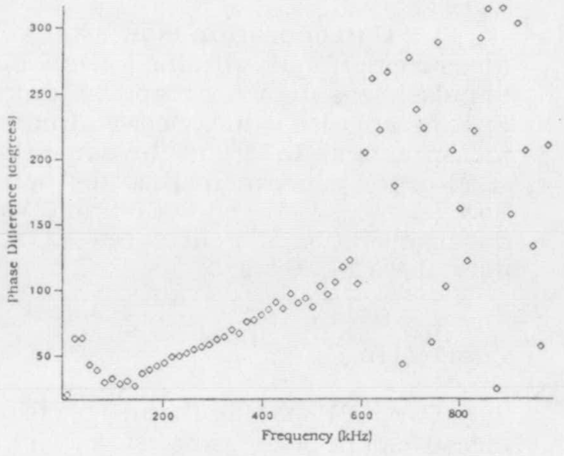

Figure 10: Phase Spectrum

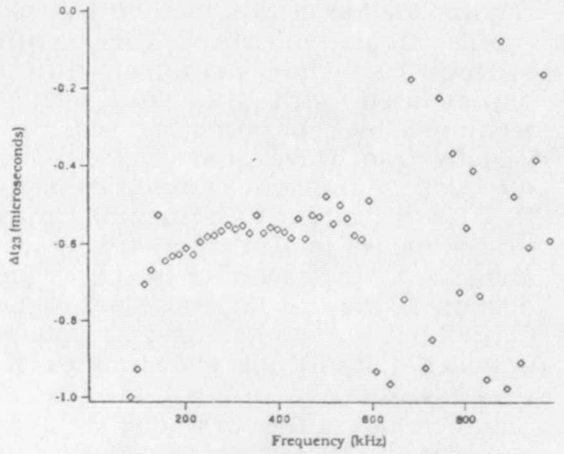

Figure 11: Time Delay Spectrum

coherence near 1 the variance of the phase angle due to the Fourier transform is negligible [5], and as mentioned previously the percentage error due to phase shifts introduced by the recording equipment was reduced to a percent or less. The contribution of aliasing error to the calculation of phase angles is also assumed to be negligible because of the strong attenuation of the emitter signal above 1 MHz [7]. At around 300 kHz the error in the frequency due to frequency averaging is about 3 percent (300 kHz ± 7.5 kHz). The uncertainty in the probe spacing is 15% (two probe radii divided by the nominal probe spacing). Analytical solutions to the equations are not available, consequently it is difficult to evaluate how these uncertainties propagate in the determination of v_f, v_ϕ, and θ. Uncertainty in those values is estimated to be about 20%.

Corroboration for the velocity measurements is obtained from specific impulse measurements made by Myers [10]. Specific impulse values derived from thrust measurements taken on the same thruster used in the experiment reported here yield flow velocities between 6000 and 7000 m/s during operation at a current of 700 A and a mass flow of 11.6 mg/s.

Conclusion

The PFVD technique for the measurement of the exhaust velocity in the near plume of a low power MPD thruster provides believable results and encourages the application of this method for velocity profile measurements. The technique surmounts the primary difficulty associciated with the Time of Flight technique by separating the plasma flow velocity from wave phase velocity. Flow direction is obtained simultaneously with the flow velocity. The use of Langmuir probes makes implementation simple, and analysis of the raw data in the frequency domain allows the dispersive nature of the plasma to be accounted for and potentially provides a multitude of estimates of the flow velocity in a single run. Shortcomings of the technique include the assumption of isotropic phase velocity and a limitation of the applicability of the method to situations where all of the receivers lie within the Mach cone of disturbances produced at the emitter.

Acknowledgements

The authors would like to express their gratitude to G. Miller and D. Tregurtha for their assistance in the laboratory. This research is supported in part by: NASA Contract No. 954997 and the Fannie and John Hertz Foundation.

References

1. Choueiri, Edgar Y. "Electron-Ion Streaming Instabilities of an Electromagnetically Accelerated Plasma", PhD Thesis, Princeton University, October 1991.
2. Boyle, Michael J. "Acceleration Processes in the Quasi-Steady Magnetoplasmadynamic Discharge", PhD Thesis, Princeton University, October 1974.
3. Tilley, Dennis L. "An Investigation of Microinstabilities in a kW Level Self-Field MPD Thruster", Master's Thesis, Princeton University, October 1991.
4. Lancaster, D. Active-Filter Cookbook, Howard W. Sams & Co., Inc., Indianapolis, 1975.
5. Bergland, G. D., "A Guided Tour of the Fast Fourier Transform", IEEE Spectrum, July 1969, pp. 41-52.
6. D. E. Smith, E. J. Powers, and G. S. Caldwell, "Fast-Fourier Transform Spectral-Analysis Techniques as a Plasma Fluctuation Diagnostic Tool", IEEE Transactions on Plasma Science, Vol. PS-2, December 1974, pp.261-272.
7. Tilley, D.L., MAE Report No. 1776.27, September/October 1990, Princeton University.
8. IMSL, Inc. Customer Relations, 2500 Permian Tower, 2500 City West Blvd. Houston, Texas 77042-3020
9. Wolfram, Stephen Mathematica: A System for Doing Mathematics by Computer, Addison-Wesley Publishing Company, Inc., 1988.
10. Myers, Roger M. "Energy Deposition in Low Power Coaxial Plasma Thrusters", PhD Thesis, Princeton University, June 1989.